

# Different Evolutionary Trajectories of Two Insect-Specific Paralogous Proteins Involved in Stabilizing Muscle Myofibrils

Nicanor González-Morales, Thomas W. Marsh, Anja Katzemich, Océane Marescal, Yu Shu Xiao, and Frieder Schöck<sup>1</sup>

Department of Biology, McGill University, Montreal, Quebec H3A 1B1, Canada

ORCID IDs: 0000-0003-1305-8992 (N.G.-M.); 0000-0002-1351-0574 (F.S.)

**ABSTRACT** Alp/Enigma family members have a unique PDZ domain followed by zero to four LIM domains, and are essential for myofibril assembly across all species analyzed so far. *Drosophila melanogaster* has three Alp/Enigma family members, *Zasp52*, *Zasp66*, and *Zasp67*. Ortholog search and phylogenetic tree analysis suggest that *Zasp* genes have a common ancestor, and that *Zasp66* and *Zasp67* arose by duplication in insects. While *Zasp66* has a conserved domain structure across orthologs, *Zasp67* domains and lengths are highly variable. In flies, *Zasp67* appears to be expressed only in indirect flight muscles, where it colocalizes with *Zasp52* at Z-discs. We generated a CRISPR null mutant of *Zasp67*, which is viable but flightless. We can rescue all phenotypes by re-expressing a *Zasp67* transgene at endogenous levels. *Zasp67* mutants show extended and broken Z-discs in adult flies, indicating that the protein helps stabilize the highly regular myofibrils of indirect flight muscles. In contrast, a *Zasp66* CRISPR null mutant has limited viability, but only mild indirect flight muscle defects illustrating the diverging evolutionary paths these two paralogous genes have taken since they arose by duplication.

**KEYWORDS** Alp/Enigma family; *Drosophila melanogaster* *Zasp67*; *Zasp66*; *Zasp52*; indirect flight muscle; myofibril assembly; PDZ; LIM

**I**NSECTS are the most successful metazoan taxon largely because of their amazing flight capabilities. Higher insects can fly exceptionally well thanks to their indirect flight muscles, which attach to the thorax and contract only minimally to indirectly move the wings via the hinge region. Some indirect flight muscles are additionally asynchronous, allowing for high frequency contractions (Deora *et al.* 2017). Such muscles require highly ordered, almost crystalline arrays of sarcomeres to contract properly by just a small percentage of their overall length.

The sarcomere is the smallest contractile unit in muscles, and many proteins contribute to the elastic and contractile properties of muscles, most notably thick filaments, which are anchored at the M-line, and thin filaments, which are

anchored at the Z-discs. Z-discs are multiprotein complexes that border the sarcomere and transmit tension during contraction, while also maintaining the structure and function of the myofibril by serving in part as signaling centers (Luther 2009; Lemke and Schnorrer 2017). In addition, Z-discs and their precursors, Z-bodies, play a crucial role in myofibril assembly. A major component of Z-discs is  $\alpha$ -actinin, which cross-links the slightly overlapping barbed ends of actin filaments at the Z-disc. Additional components include proteins of the Alp/Enigma family, which function in the maintenance of Z-discs, and have also been shown to play an important role in myofibril assembly. These proteins share a unique N-terminal PDZ domain containing a conserved PWGFRL motif required for  $\alpha$ -actinin binding, and zero to four C-terminal LIM domains (Katzemich *et al.* 2013; Liao *et al.* 2016). PDZ domains are found in prokaryotes and eukaryotes, whereas LIM domains are restricted to eukaryotes. Both domains mediate a wide variety of protein–protein interactions (Kadrmars and Beckerle 2004; Koch *et al.* 2012; Luck *et al.* 2012). In vertebrates, the Alp/Enigma family comprises three Enigma family members, which have an N-terminal PDZ domain and

Copyright © 2019 by the Genetics Society of America

doi: <https://doi.org/10.1534/genetics.119.302217>

Manuscript received March 11, 2019; accepted for publication May 7, 2019; published Early Online May 13, 2019.

Supplemental material available at FigShare: <https://doi.org/10.25386/genetics.8001722>.

<sup>1</sup>Corresponding author: Department of Biology, McGill University, 1205 Docteur Penfield Ave., Montreal, QC H3A 1B1, Canada. E-mail: [frieder.schoeck@mcgill.ca](mailto:frieder.schoeck@mcgill.ca)

three C-terminal LIM domains (ZASP/Cypher/Oracle/LDB3/PDLIM6, ENH/PDLIM5, and PDLIM7/ENIGMA/LMP-1) and four Alp family proteins that contain one N-terminal PDZ domain with only one C-terminal LIM domain (CLP36/PDLIM1/Elfin/hCLIM1, PDLIM2/Mystique/SLIM, ALP/PDLIM3, and RIL/PDLIM4) (Faulkner *et al.* 1999; Vallenius *et al.* 2000; Jo *et al.* 2001; Pashmforoush *et al.* 2001; Zhou *et al.* 2001; Torrado *et al.* 2004; Vallenius *et al.* 2004; Cheng *et al.* 2010; Zheng *et al.* 2010; D’Cruz *et al.* 2016). In *Drosophila*, Zasp52 has a PDZ, ZM (Zasp-like motif) and four LIM domains; while Zasp66 and Zasp67 feature only the N-terminal PDZ domain and a weakly conserved ZM domain. Zasp52 colocalizes with  $\alpha$ -actinin at Z-discs and plays a role in myofibril assembly and maintenance (Jani and Schöck 2007; Chechenova *et al.* 2013; Katzemich *et al.* 2013). Many different Zasp52 splice isoforms have been identified, resulting in up to 61 different proteins, some of which are restricted to specific muscle types (Katzemich *et al.* 2011; Brown *et al.* 2014). Furthermore, RNAi-mediated knockdown indicates that Zasp52, Zasp66, and Zasp67 cooperate in myofibril assembly and play partially redundant roles at the Z-disc (Katzemich *et al.* 2013). Mutations of Zasp52 orthologs in vertebrates cause similar defects, ranging from improper formation of somites and heart in zebrafish to fragmented Z-discs in skeletal and cardiac muscles in mice (Zhou *et al.* 2001; van der Meer *et al.* 2006; Cheng *et al.* 2010). Similar to *Drosophila*, a ZASP/Cypher and ENH double knock-out in mice demonstrates partial redundancy in myofibril assembly (Mu *et al.* 2015). A knockdown of the single *Caenorhabditis elegans* ortholog ALP-1 displays defects in actin filament organization, but motility defects are much milder than in vertebrates or *Drosophila* (McKeown *et al.* 2006; Han and Beckerle 2009; Nahabedian *et al.* 2012). Mutations in the human ortholog ZASP result in phenotypes of variable severity from congenital myopathy with fetal lethality to late-onset cardiomyopathy (Sheikh *et al.* 2007; Shieh 2013).

By necessity, the large majority of cytoskeletal proteins are common to all muscle types to ensure basic assembly and functionality of sarcomere contractility. Much less is known about proteins required for the assembly of specific muscle types. To better understand potential muscle type-specific proteins, we analyzed the function of Zasp66 and Zasp67 proteins. Phylogenetic tree analysis indicates that Zasp66 and Zasp67 are duplications of Zasp52. We show that Zasp67 is found only in some higher insect orders and appears to have an expression restricted to indirect flight muscles in *Drosophila melanogaster*, where it colocalizes with Zasp52 at Z-discs. In contrast, Zasp66 is found in all insects and is expressed equally in all muscle types in *D. melanogaster*. A CRISPR null mutant of *Zasp67* is viable and flightless. *Zasp67* mutants show extended and broken Z-discs in adult flies only, indicating that the protein helps stabilize the highly regular myofibrils of indirect flight muscles. In contrast, the CRISPR null mutant of *Zasp66* shows high pupal lethality consistent with its wide-ranging expression in all muscle types but has

only minor effects on indirect flight muscle organization. This work illustrates the different evolutionary trajectories taken by two paralogous genes.

## Materials and Methods

### *Inferring homologous genes from 1Kite database in insect species*

Single isoforms of Zasp52 (NP\_001027420.2), Zasp66 (NP\_729395.2), Zasp67 (NP\_648358.2) and  $\alpha$ -actinin (NP\_477485.1) were compared to the 1Kite insect species database using TSA\_BLAST. Only species publicly available at the time were included in the analysis. We recovered all possible homologous hits (BLAST cut-off = 0.1). Then, the retrieved hits were compared to the *D. melanogaster* transcriptome refseq\_rna database using BLAST. “Candidate orthologs” were defined as those hits, that when compared back to the *D. melanogaster* transcriptome, would result in the original gene used for the first BLAST query. This approach filters out non-Zasp genes with conserved PDZ or LIM domains and distinguishes the orthologs from individual Zasp genes. We then made a list of the species in which orthologs were found from the BLAST output, and compared it with a list of all the species found in the 1kite database. Finally, the results were plotted next to a current phylogenetic tree model (Misof *et al.* 2014). Data handling was done using R software. Commands from the following packages were used: “splitstackshape,” “plyr,” “tidyr,” “plotrix” and “ape” (Gentleman *et al.* 2004; Paradis *et al.* 2004).

### *Insect Zasp67 homologs using the NCBI nr protein database*

A similar strategy as described above was used to fetch Zasp67 orthologs from the NCBI nonredundant protein database. The amino acid sequence of a single Zasp67 isoform (NP\_648358.2) was used as query (BLASTp) and the entire nonredundant protein database as subject. The resulting hits were filtered by comparing them back to the *D. melanogaster ref\_seq* protein database and selecting only the ones resulting in Zasp67 as the highest score hit. Finally, the protein sequences from the retrieved Zasp67 orthologs were analyzed using the Conserved Domain Database (CDD) Search from NCBI (Marchler-Bauer *et al.* 2015).

### *Phylogenetic tree building*

The amino acid sequences from Zasp52, Zasp66, and Zasp67 orthologs from different species and from the three *D. melanogaster* PDZ-containing proteins Scrib (Scribbled), Pyd (Polychaetoid), and Dysc (Dyschronic) were aligned using COBALT (Papadopoulos and Agarwala 2007). We then restricted the alignment to the conserved region containing the PDZ domain. Finally, we estimated the phylogeny using PHYML through the T-REX server (Guindon and Gascuel 2003; Boc *et al.* 2012). The initial tree was inferred with

BioNJ, readjustments were done with PHYML, and branch support was estimated using nonparametric bootstrap analysis with 1000 replicates.

### **Analysis of the correlated expression and the developmental expression of *Zasp* genes in *Drosophila* using Modencode data**

The mRNA expression data for all three *Zasp* genes was downloaded directly from Flybase as reads per kilobase of exon model per million mapped reads (RPKM) (Graveley *et al.* 2011; Marygold *et al.* 2016). Then, the RPKM values between two genes were compared using scatter plots and the correlation coefficient was calculated. Plots and calculations were done in R software.

### **Adult muscle dissections**

Indirect flight muscle dissections were done as previously described (González-Morales *et al.* 2017; Xiao *et al.* 2017). Briefly, flies were dissected in 100  $\mu$ l of ice-cold Relaxing-Glycerol solution [20 mM sodium phosphate buffer, 5 mM MgCl<sub>2</sub>, 5 mM EGTA, 5 mM ATP, 5 mM DTT, protease inhibitor, glycerol 1:1 (v/v)]. Abdomens were removed before halving thoraces. Halved thoraces were placed in Relaxing-Glycerol solution and stored for 12 hr at  $-20^{\circ}$ . Thoraces were then fixed in 4% formaldehyde for 1 hr at room temperature and subsequently washed with PBS containing 0.3% Triton (PBT). Muscle fibers were isolated from fixed thoraces and allowed to incubate for 1 hr in fluorescently labeled phalloidin (Alexa Fluor 488 phalloidin, 1:500), before washing with PBT. Stained muscle fibers were then mounted on a microscope slide and preserved using ProLong Gold antifade reagent (Thermo Fisher Scientific) until imaging. Other adult muscles were prepared similarly. Pupal dissections were carried out as previously described (Katzemich *et al.* 2012).

### **Imaging and Z-disc phenotype counting**

Fluorescence images were acquired using a Leica SP8 point-scanning confocal system with a 63 $\times$ /1.4 oil objective. Muscle fiber images were processed and analyzed using Fiji/ImageJ (Schindelin *et al.* 2012). The total number, number of abnormal, number of extended, and number of broken Z-discs were counted for each image. Normal Z-discs were defined as straight, continuous bars (Supplemental Material, Figure S3A). Abnormal Z-discs were classified as either extended or broken. Z-discs with extensions continuously connected to the main core of the Z-disc were counted as extended Z-discs (Figure S3B). The extended disc classification included linked Z-discs, a commonly seen formation of two or more Z-discs connected by thin strands originating from the cores. Broken Z-discs were defined as any Z-disc with a break in the continuity of the Z-disc core (Figure S3C). When a Z-disc was both “broken” and “extended”, it was counted as broken.

### **Flight and climbing assays**

After CO<sub>2</sub> anesthesia, flies were left to recover for a minimum of 4 hr before being tested. All tested flies were at least 2 days old. Climbing was assessed in plastic vials. Single flies were placed into tubes and tapped to bring the fly to the bottom. Once the fly began to climb up the vial wall, a 3 sec timer was started, and the final position of the fly was recorded. The climbing assay was performed three times per fly and the maximum value was used for statistics. For flight assays, individual flies were released from a plastic vial: if it flew upwards it was marked as a flyer, whereas if it fell or glided to the ground it was marked as a nonflyer. Samples of different sets of 30 flies were used to calculate the SE.

***Drosophila* genetics:** Flies were maintained at 25 $^{\circ}$  on standard cornmeal/agar food, and handled using standard fly stations. As a marker for the Z-disc we used *Zasp52-MI02988-mCherry*, a replacement of the *Zasp52-MI02988* cassette (BDSC #41034) with the mCherry CDS inframe and flanked by exon acceptor/donor sequences (Venken *et al.* 2011; Xiao *et al.* 2017). *Zasp52-MI02988-mCherry* should label 19 out of 21 FlyBase-predicted isoforms. To rescue the *Zasp67* mutant phenotype and to analyze *Zasp67* expression and localization, we used a fosmid-based duplication that contains the *Zasp67* gene with a C-terminal 2xTY1-SGFP-V5-preTEV-BLRP-3xFLAG tag (VDRC #318355) (Sarov *et al.* 2016). We refer to this strain as *Zasp67-GFP*. *Zasp67-GFP* should label three out of four FlyBase-predicted isoforms. The deficiency *Df(3L)BSC393* deletes *Zasp67* (BDSC #24417) (Cook *et al.* 2012). The recombinant stock carrying both the *Zasp67* mutant and *Zasp67-GFP* rescue was generated by standard recombination crosses.

To rescue the *Zasp66* mutant phenotype, we used a bacterial artificial chromosome-based duplication that contains the entire *Zasp66* gene (BAC:CH322-127P23). We obtained the BAC from the BACPAC Resources Center at the Children’s Hospital Oakland Research Institute. We then confirmed the BAC by restriction digests and end sequencing. Finally, we made a transgenic fly stock by incorporating the BAC into the second chromosome at the *M{3xP3-RFP.attP}ZH-58A* landing site. We refer to this strain as *Zasp66-BAC*.

### **Generation of *Zasp66* and *Zasp67* null mutants**

Both *Zasp66* and *Zasp67* null mutants were made using CRISPR-mediated homology-directed repair. The *Zasp67* null mutant is a 1736 bp deletion allele of *Zasp67*, that replaces exons 2, 3, and 4 of the *Zasp67* gene with a cassette containing an attP site, a Gal4::VP16 fusion gene and a *w*<sup>+</sup> selection marker. The *Zasp66* null mutant is a 4239-bp deletion allele that replaces exon 2, 3, 4, and part of exon 5 with the same cassette. We forced the simultaneous cleavage of two sites flanking the desired deletions, by coexpression of two gRNAs

(Kondo and Ueda 2013). The Zasp67 upstream gRNA sequence GATATCGCCGATTAGATG[CGG], the Zasp67 downstream gRNA sequence TGCATTCACTCACTCACCAT[TGG], the Zasp66 upstream gRNA sequence CACCGCAAACCTCATGCAGCT [TGG], and the Zasp66 downstream gRNA sequence GGCTGCTCCTTGTAGTAGAC[TGG] were cloned into a U6 promoter plasmid. The replacement cassettes together with two 1 kb homology arms were cloned into pUC57-Kan vectors and used as donor templates for homology-directed repair. The two gRNAs and the donor plasmid were coinjected into *w*[1118]; *attP40{nos-Cas9}/CyO* embryos. The resulting flies were outcrossed, and the offspring carrying a *w*<sup>+</sup> selection marker were selected. The desired mutations were then validated by genomic PCR and sequencing. The mutagenesis projects were performed with the help of Wellgenetics. We used the following oligonucleotides for PCR validation:

**Zasp67 exon 2 blue:** OWG4141 ACTTCTACTCGAGCACCCCT.  
OWG4142 AAGGATGGGAAAGCTCACCG.

**Zasp67 exon 4 green:** OWG4143 GCGGGCGAGTCTTTTAACC.  
OWG4144 TTCCGGCTGTCACACGTAAA.

**Zasp67 up PCR red:** OWG1824 CCATCGTGTCTTACTGTTTATTGCC.  
OWG6830 CAAGTTGCGGGTAGGAAAAA.

**Zasp67 down PCR magenta:** OWG6829 AACGGAAACGA  
AAACAATCG.  
OWG1703 TCGGTTTTCTTTGGAGCAC.

**Zasp66 up PCR red:** OWG5106 ATCCGCTCAAGGCTGATCTA.  
OWG1703 TCGGTTTTCTTTGGAGCAC.

**Zasp66 down PCR magenta:** OWG5107 CACAAGTTCTGCT  
GCAGTG.  
OWG1824 CCATCGTGTCTTACTGTTTATTGCC.

### Data availability

All *Drosophila* strains and materials generated in this study are available upon request. The authors affirm that all data necessary for confirming the conclusions of the article are present within the article, figures, and supplemental figures and tables. Table S1 lists the accession numbers of 1Kite genomes analyzed (related to Figure 1A). Table S2 lists the accession numbers of proteins used to estimate Zasp phylogeny (related to Figure 1B). Table S3 lists the accession numbers of Zasp66 and Zasp67 orthologs (related to Figure 2C). Figure S1 shows a radial phylogenetic tree of insect species with Zasp orthologs highlighted (related to Figure 1A). Figure S2 shows Zasp52 localization in a *Zasp67* mutant (related to Figure 6). Figure S3 shows a quantification of the *Zasp67* indirect flight muscle phenotype (related to Figure 6). Supplemental material available at FigShare: <https://doi.org/10.25386/genetics.8001722>.

## Results

### *Zasp66 and Zasp67 are duplications occurring only in insects*

We previously showed that Zasp52, Zasp66, and Zasp67 are similar to human Alp/Enigma proteins, but did not investigate the evolutionary history of this family (Katzemich *et al.* 2013). We therefore first sought to discover which species have candidate orthologs of Zasp52, Zasp66, and Zasp67. We searched DNA and protein sequence databases with *D. melanogaster* Zasp52, Zasp66, Zasp67, and  $\alpha$ -actinin sequences as input. Zasp52 and  $\alpha$ -actinin orthologs occur in all metazoans, and predate the evolutionary appearance of muscles (Steinmetz *et al.* 2012). Zasp66 orthologs are restricted to insects. Zasp67 orthologs are even more limited in distribution and can only be found in insects with indirect flight muscles (Figure 1A, Figure S1, and Table S1). The fact that we found Zasp52 in all species analyzed indicates that the absence of Zasp66 or Zasp67 in a given genome is likely not attributable to low genome quality. To confirm orthology, we chose representative Zasp members from each insect order and built a phylogenetic tree with their PDZ domains plus the PDZ domains of three closely related proteins from *D. melanogaster* (Figure 1B and Table S2). The phylogenetic tree supports our Zasp annotation, because they form distinct and well-supported clades. In addition, Zasp52 and Zasp67 appear to be more closely related to each other than to Zasp66 (Figure 1B). These data suggest that Zasp66 and Zasp67 arose by duplication of Zasp52 in insects, with Zasp66 arising first. This is consistent with the more widespread distribution of Zasp66 (Figure 1A).

Sometimes duplicated genes acquire specific functions. To test if any of the three Alp/Enigma genes in flies has acquired a novel function, we first compared the mRNA expression profiles at different developmental stages of Zasp52, Zasp66, and Zasp67 using Modencode mRNA datasets. While Zasp52 and Zasp66 have highly correlated expression profiles (Spearman correlation = 0.86), the expression of Zasp67 is correlated with neither Zasp52 nor Zasp66 (Figure 2A; Spearman correlation = 0.48 and 0.34). These relationships can be better seen when the expression profiles of these three genes are plotted over developmental time. Whereas Zasp52 and Zasp66 are coexpressed during embryonic and larval body wall muscle development, as well as adult muscle development, Zasp67 is exclusively expressed during adult muscle development (Figure 2B). The expression profiles suggest that both paralogs carry out distinct functions in *Drosophila*.

We also analyzed the length variation and domain composition of Zasp66 and Zasp67 orthologs. In contrast to Zasp66, Zasp67 orthologs vary widely in length and protein domain composition in different species (Figure 2, C and D and Table S3). For example, while close to 90% of Zasp66 orthologs have a PDZ domain and a ZM motif (also called DUF4749), only 18% of Zasp67 orthologs have a ZM motif (Figure 2C). In addition, we found 38 different domains

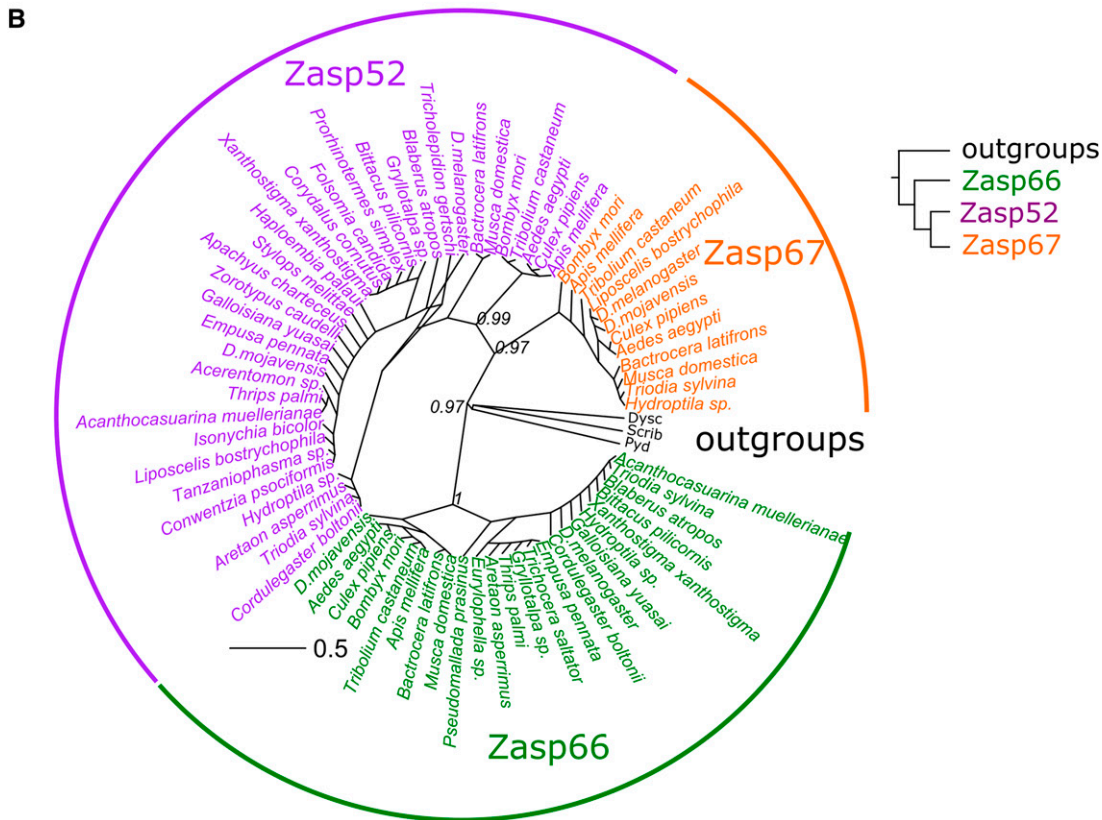
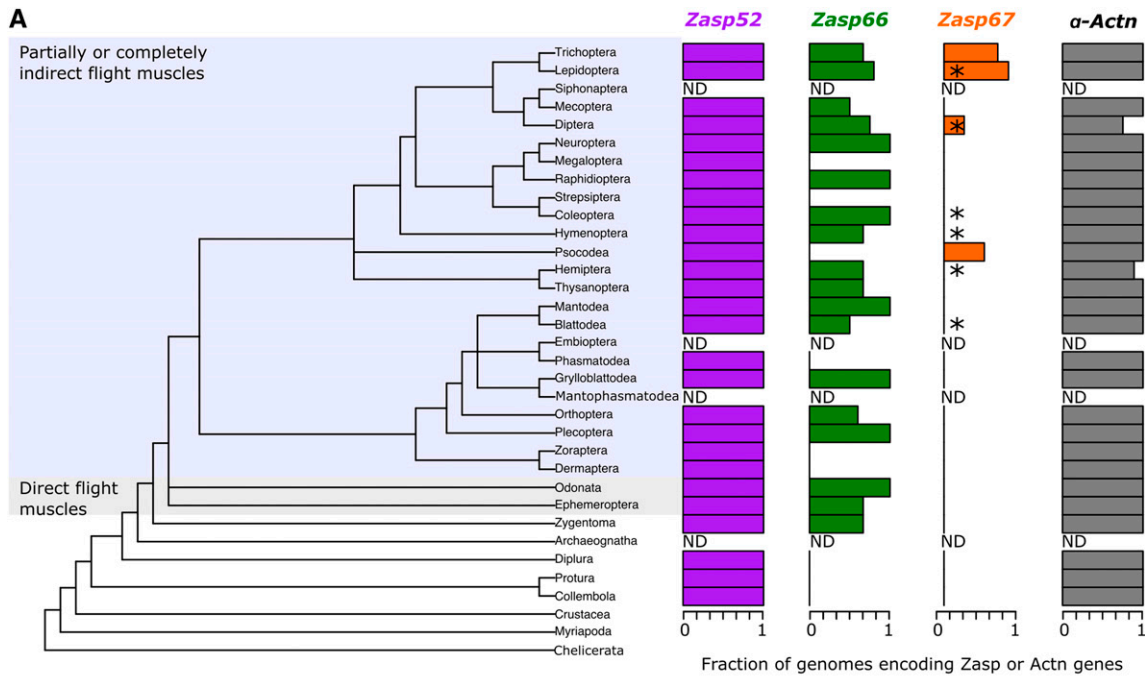


**Figure 1** Phylogeny of Zasp proteins. (A) Phylogenetic tree of insects based on Misof *et al.* (2014). Insects with partially or completely indirect flight muscles and insects with direct flight muscles only are highlighted. Branch names indicate the insect order (left panel). Bar plots indicate the relative number of orthologs found per insect order in the 1Kite database. ND: no whole genome sequence data available. The asterisks on the *Zasp67* bar plot denote orthologs found in the NCBI nonredundant protein database. The y-axis of the plots matches the branch name from the phylogenetic tree. Accession numbers are provided in Table S1. (B) Radial phylogenetic tree of the PDZ domain regions of Zasp proteins with bootstrap support values. *Zasp52* (magenta), *Zasp66* (green), and *Zasp67* (orange) orthologs from selected species are shown as tip labels. The PDZ regions from three closely related non-Zasp proteins (Polychaetoid-Pyd, Scribbled-Scrib, and Dyschronic-Dysc) from *Drosophila melanogaster* were used as outgroups and are shown in black. Numbers next to the tree nodes denote the bootstrap support value. The distance scale represents the number of amino acid changes per site. The simplified tree on the right summarizes the phylogenetic relationships. Accession numbers are provided in Table S2.

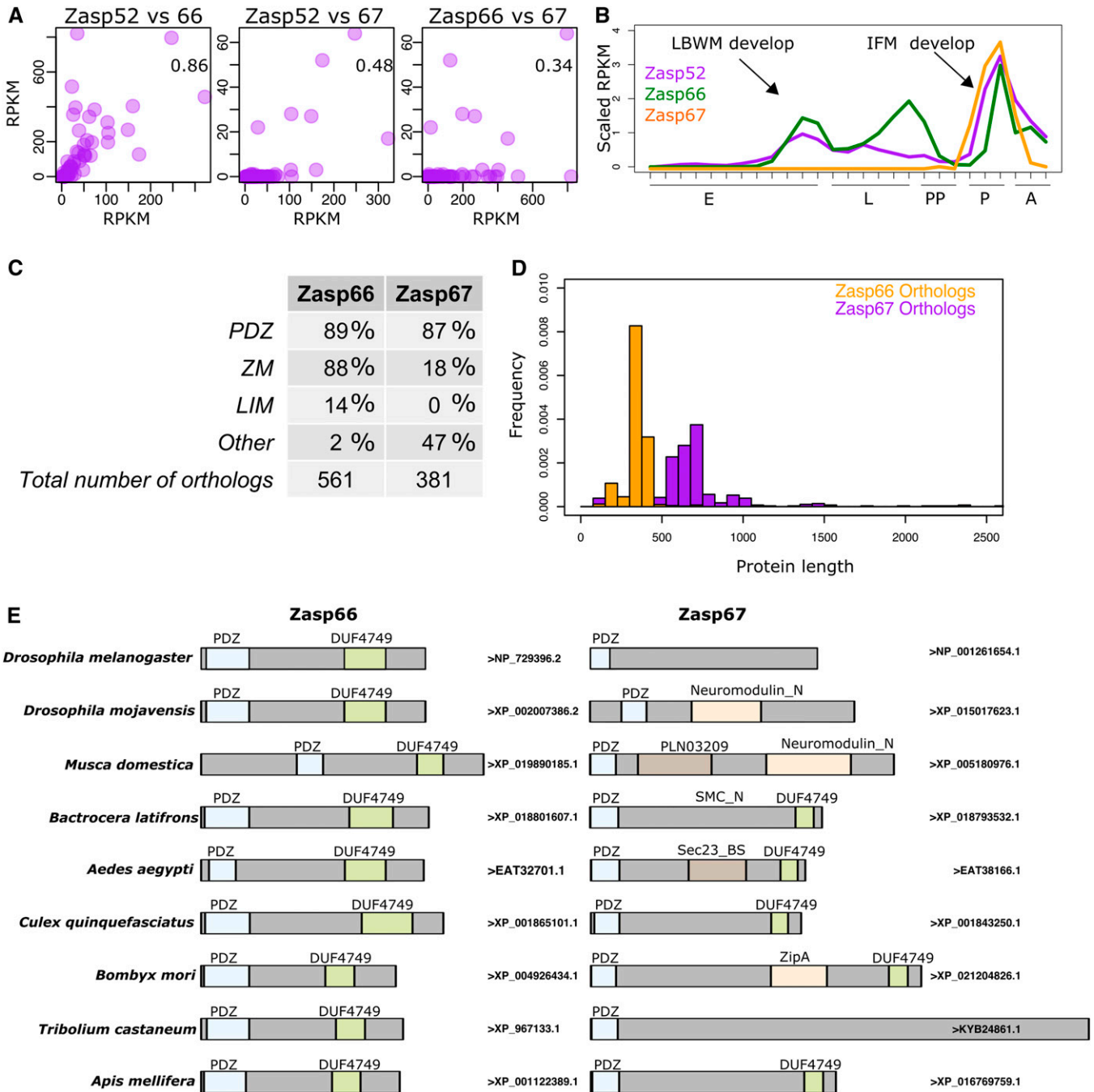


**Figure 2** Zasp67 orthologs encode highly variable proteins. (A) Scatterplots of mRNA expression data from the Modencode project comparing the three Zasp genes to each other. The expression of *Zasp52* and *Zasp66* correlates (left panel). The expression of *Zasp67* does not correlate with *Zasp52* or *Zasp66* (middle and right panels). Spearman rank correlation values are shown. RPKM, reads per kilobase of exon model per million mapped reads. (B) A plot of the relative expression (scaled RPKM) of all three Zasp genes against developmental time. E, embryonic stage; L, larval stage; PP, prepupal stage; P, pupal stage; A, adult; LBWM, larval body wall muscle; IFM, indirect flight muscle. *Zasp67* expression is restricted to the pupal stages when IFM develop. (C) Table of all protein domains found associated with *Zasp66* and *Zasp67* orthologs. Accession numbers are provided in Table S3. (D) Histogram of *Zasp66* and *Zasp67* ortholog length frequencies. (E) Examples of *Zasp66* and *Zasp67* orthologs.

present in some *Zasp67* orthologs that are not commonly associated with Alp/Enigma family members and are not found in *Zasp66* orthologs (Figure 2, C and E). This suggests that *Zasp67* orthologs have acquired novel functions in different insect lineages.

To further explore this hypothesis, we compared closely related *Zasp66* and *Zasp67* orthologs. Variable domain composition happens even between closely related species for *Zasp67*, but never for *Zasp66* (Figure 2E). Whereas the *Zasp67* proteins of most *Drosophila* species have a PDZ

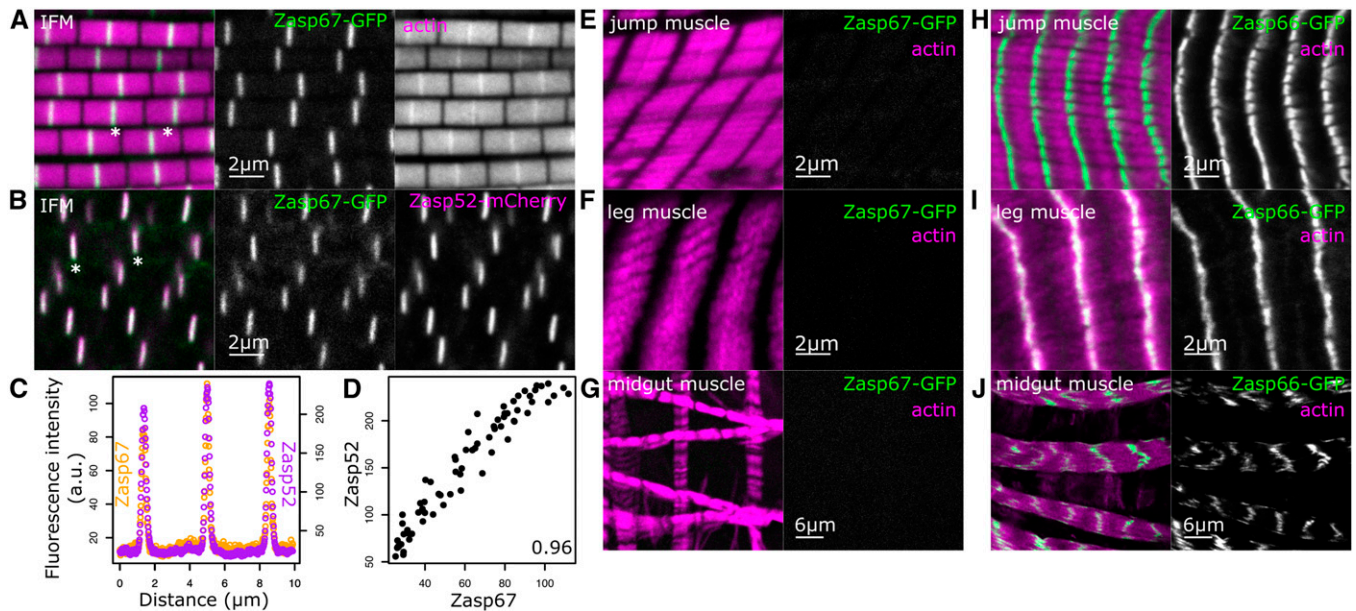


**Figure 3** Zasp67 expression is restricted to indirect flight muscles, where it localizes to Z-discs. (A) Confocal image of indirect flight muscles from *Zasp67-GFP* flies stained with phalloidin to visualize actin filaments (magenta in merged image). GFP fluorescence is shown in green (appearing white when overlapping with magenta in merged image). (B) Confocal image of indirect flight muscles from flies with *Zasp67-GFP* and *Zasp52-mCherry* alleles. Asterisks are drawn in (A and B) below selected Z-discs. (C) Profile plot of Zasp67 and Zasp52 fluorescence from a line extending over three Z-discs in (B). (D) Scatterplot of Zasp67 and Zasp52 fluorescence data from (B), with Pearson's correlation value indicated. (E–J) Confocal images of jump muscles, leg muscles, and midgut muscles. Left panels show the merge of actin staining in magenta and GFP in green, right panels show only GFP. (E–G) Different adult muscles from *Zasp67-GFP* flies. (H–J) Different adult muscles from *Zasp66-GFP* flies. Bars are shown. IFM, indirect flight muscle.

domain, *Drosophila mojavensis* Zasp67 features an additional C-terminal neuromodulin domain. The Zasp67 orthologs from two studied mosquito species are also divergent. Both contain a PDZ domain and a ZM/DUF4749 domain, but *Aedes aegypti* Zasp67 contains an additional Sec23\_beta sandwich domain (Figure 2E). In contrast, the Zasp66 orthologs have the same protein domain composition and arrangement in most species analyzed (Figure 2E). These data highlight the variability of Zasp67 orthologs compared to Zasp66.

#### **Zasp66 and Zasp67 expression and localization**

We then explored fly Zasp66 and Zasp67 function in more detail. First, we asked if Zasp67 expression and localization is similar to Zasp52 and Zasp66 (Katzemich *et al.* 2013; Liao *et al.* 2016). We analyzed indirect flight muscles for Zasp67 expression and localization with a fosmid-based duplication of the *Zasp67* locus containing a C-terminal fusion of GFP to Zasp67 (Figure 3, A–D). Zasp67-GFP is strongly expressed in indirect flight muscles and localizes to Z-discs (Figure 3, A and B). Zasp67 localization fully overlaps with Zasp52 at Z-discs, which can be seen by plot profiles and intensity correlation measurements (Figure 3, C and D). We also analyzed a range of other adult muscles including the jump muscle, leg muscle, and midgut muscle. None of these muscles show any Zasp67 expression (Figure 3, E–G), indicating that Zasp67 expression appears to be restricted to indirect flight muscles. In contrast, Zasp66, which also colocalizes with Zasp52 at the Z-discs of indirect flight muscles (Katzemich *et al.* 2013), is

additionally found at Z-discs of all other muscles we analyzed (Figure 3, H–J). This further confirms the similar spatial expression of Zasp66 and Zasp52.

#### **A CRISPR null mutant of Zasp67 is flightless**

To investigate the function of Zasp67, we generated a null mutant using CRISPR-mediated homology-directed repair. We replaced three N-terminal exons containing the PDZ domain of Zasp67 with a dominant genetic marker (Figure 4A). This knock-out deletes all annotated isoforms of *Zasp67* and was verified by various genomic PCRs testing for cassette insertion and exon deletion (Figure 4B). We next assayed the flying ability of *Zasp67* mutants. In contrast to wild type (Oregon R), *Zasp67* homozygotes are flightless. *Zasp67* mutants transheterozygous over the deficiency *Df(3L)BSC393*, which deletes *Zasp67*, are equally flightless, indicating that our *Zasp67* mutant is indeed a null mutant, and that the flightless phenotype is caused by a mutation in *Zasp67* (Figure 4C). Control flies *Zasp67/+*, *Df(3L)BSC393/+*, and *Zasp67-GFP/+* have flying capabilities similar to wild-type flies (Figure 4C). Finally, we can largely rescue flight defects of *Zasp67* homozygotes and *Zasp67/Df(3L)BSC393* transheterozygotes by re-expressing Zasp67 with the fosmid-based *Zasp67-GFP* fusion transgene (Figure 4C). This confirms that the flightless phenotype is caused by the *Zasp67* mutation. Additionally, it indicates that the GFP tag does not interfere with Zasp67 function. Using the same genotypes, we also assessed climbing ability of *Zasp67* flies, but could not detect statistically significant differences between wild type, *Zasp67*

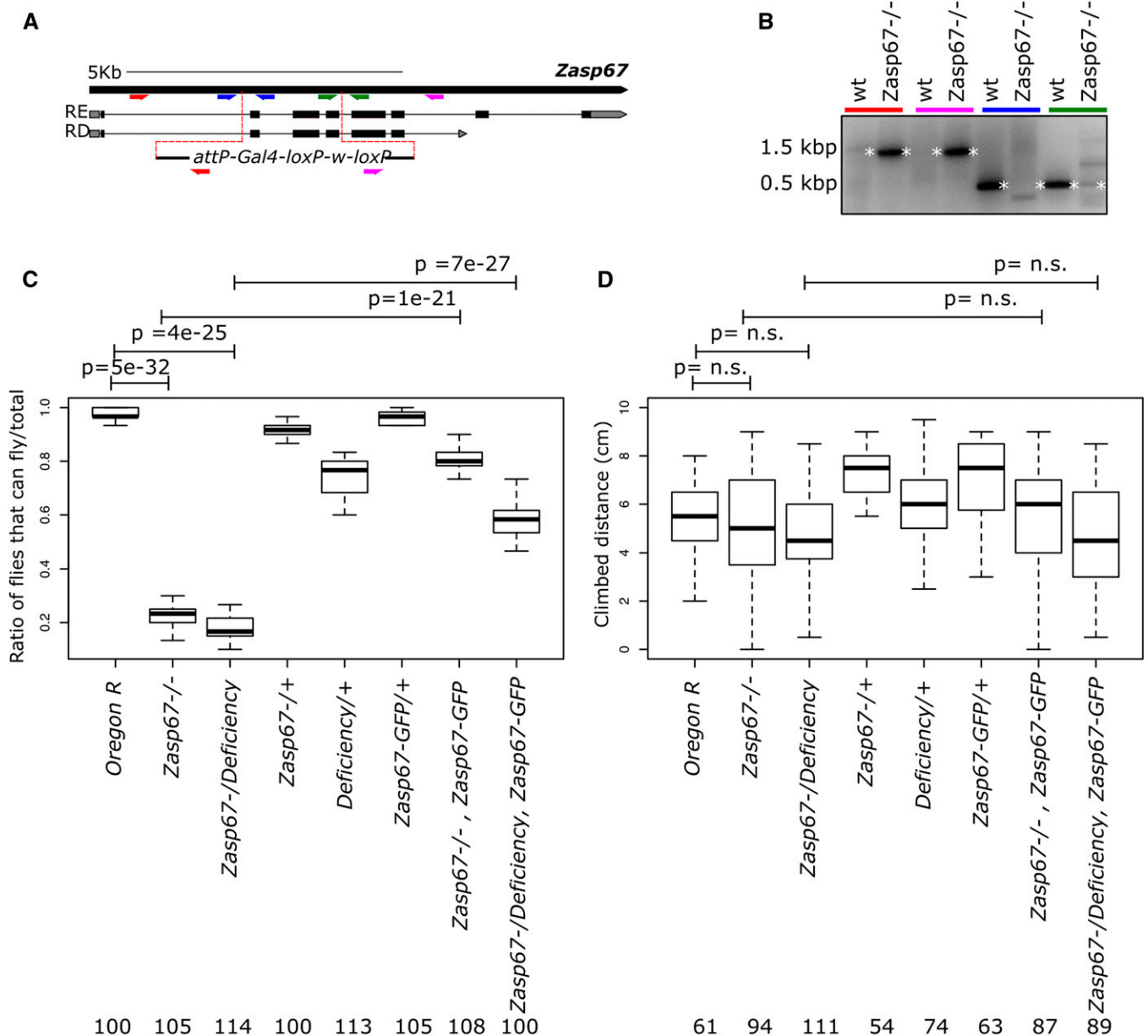


**Figure 4** The *Zasp67* null mutant flies are flightless. (A) Cartoon of *Zasp67* genomic locus with selected transcripts. The gRNA-targeted break points are shown as red dotted lines. The replacement cassette is shown at the bottom. Primer pairs used for validation of the mutant are shown in different colors. (B) Ethidium bromide-stained agarose gel of PCR products obtained from *Zasp67* homozygous mutant flies and wild-type (wt) flies. The colored lines at the top of the gel correspond to the primer pairs drawn in (A). (C) Boxplots of the ratio of flies able to fly in different genetic backgrounds. (D) Boxplots of the climbing distance in flies with different genetic backgrounds. The *P*-values were adjusted by Bonferroni correction and are shown for selected genotype pairs. Number of flies tested is given for each genotype.

mutant, and *Zasp67* expressing *Zasp67*-GFP (Figure 4D). The absence of climbing defects is consistent with the lack of expression of *Zasp67* in leg and jump muscles.

#### A CRISPR null mutant of *Zasp66* shows high pupal lethality

To better investigate the function of *Zasp66*, we also generated a null mutant using CRISPR-mediated homology-directed

repair. We replaced six N-terminal exons encoding the PDZ and ZM domain of *Zasp66* with a dominant genetic marker (Figure 5A). This knock-out deletes all annotated isoforms of *Zasp66* and was verified by genomic PCRs confirming cassette insertion (Figure 5B). The *Zasp66* null mutation affects neither flying nor climbing ability of flies surviving to adulthood (Figure 5, C and D). However, the *Zasp66* mutant shows high pupal lethality, consistent with the ubiquitous expression of

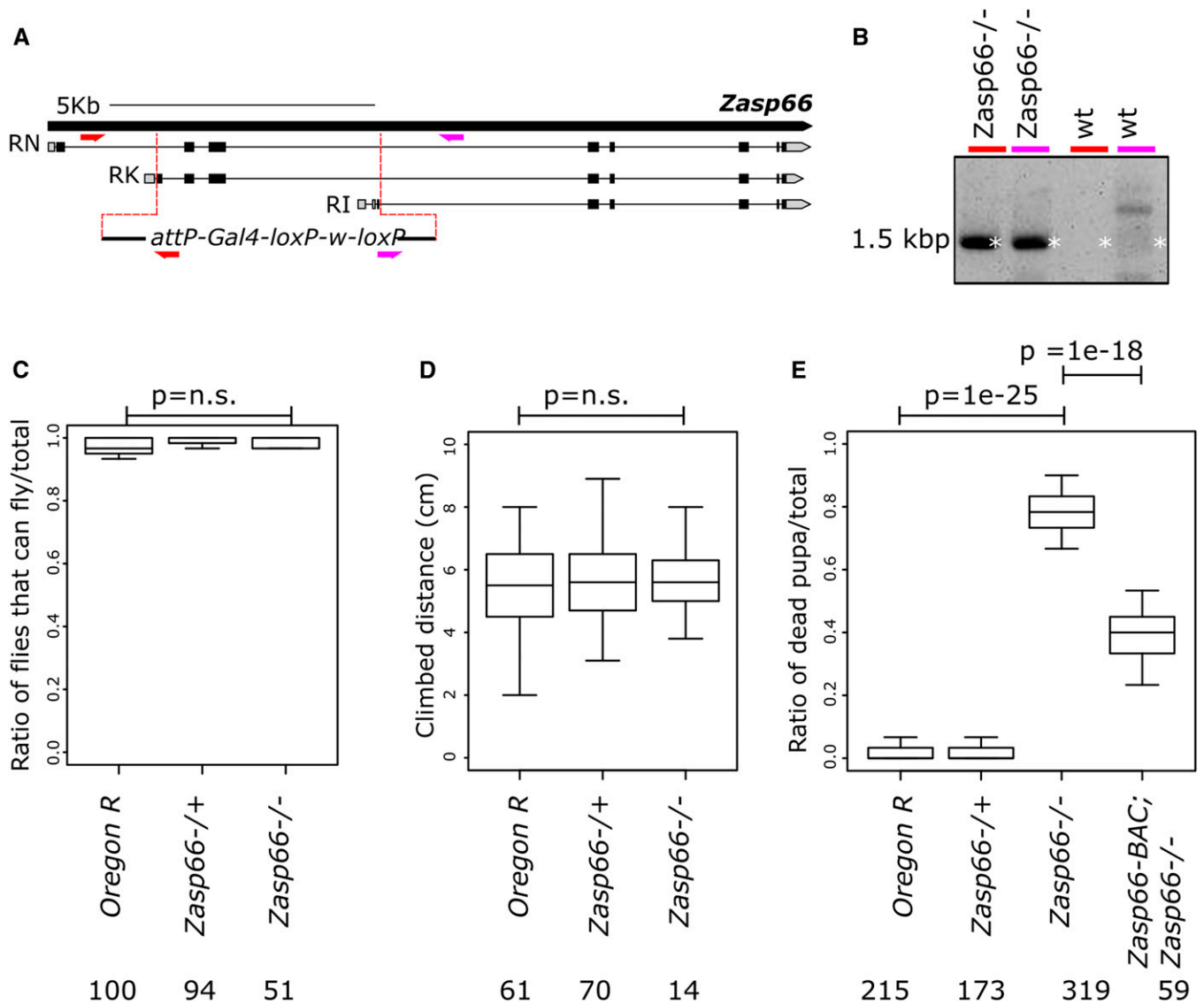


**Figure 5** The *Zasp66* null mutant flies show high pupal lethality. (A) Cartoon of *Zasp66* genomic locus with selected transcripts. The gRNA-targeted break points are shown as red dotted lines. The replacement cassette is shown at the bottom. Primer pairs used for validation of the mutant are shown in different colors. (B) Ethidium bromide-stained agarose gel of PCR products obtained from *Zasp66* homozygous mutant flies and wild-type (wt) flies. The colored lines at the top of the gel correspond to the primer pairs drawn in (A). (C) Boxplots of the ratio of flies able to fly in different genetic backgrounds. (D) Boxplots of the climbing distance in flies with different genetic backgrounds. (E) Boxplots of the ratio of dead pupae in different genetic backgrounds. The *P*-values were adjusted by Bonferroni correction and are shown for selected genotype pairs. Number of flies tested is given for each genotype.

*Zasp66* in muscles (Figure 5E). In addition, pupal lethality can be partially rescued by *Zasp66*-BAC, demonstrating that *Zasp66* is responsible for the observed phenotype (Figure 5E).

#### ***Zasp67* mutants have defective indirect flight muscle myofibrils**

The indirect flight muscles of *Zasp67* mutants were also analyzed using confocal microscopy to determine if there are visible structural defects. Myofibrils of wild type indirect flight muscles are highly regular structures with identical sarcomere width and length and identical Z-disc size (Figure

6A). In contrast, *Zasp67* mutant myofibrils or *Zasp67/Df(3L) BSC393* mutant myofibrils exhibit substantial structural defects ranging from split myofibrils to extended or broken Z-discs (Figure 6, B and C). These phenotypes are fully rescued by re-expressing *Zasp67-GFP* (Figure 6D). Furthermore, there are no changes to *Zasp52* levels or localization in *Zasp67* mutants, indicating that *Zasp52* does not appear to be upregulated in response to an absence of *Zasp67* (Figure S2). In contrast, the *Zasp66* indirect flight muscle phenotype is considerably milder, with few obvious defects visible at the confocal microscopy level (Figure 6E), in line with its normal flight behavior.

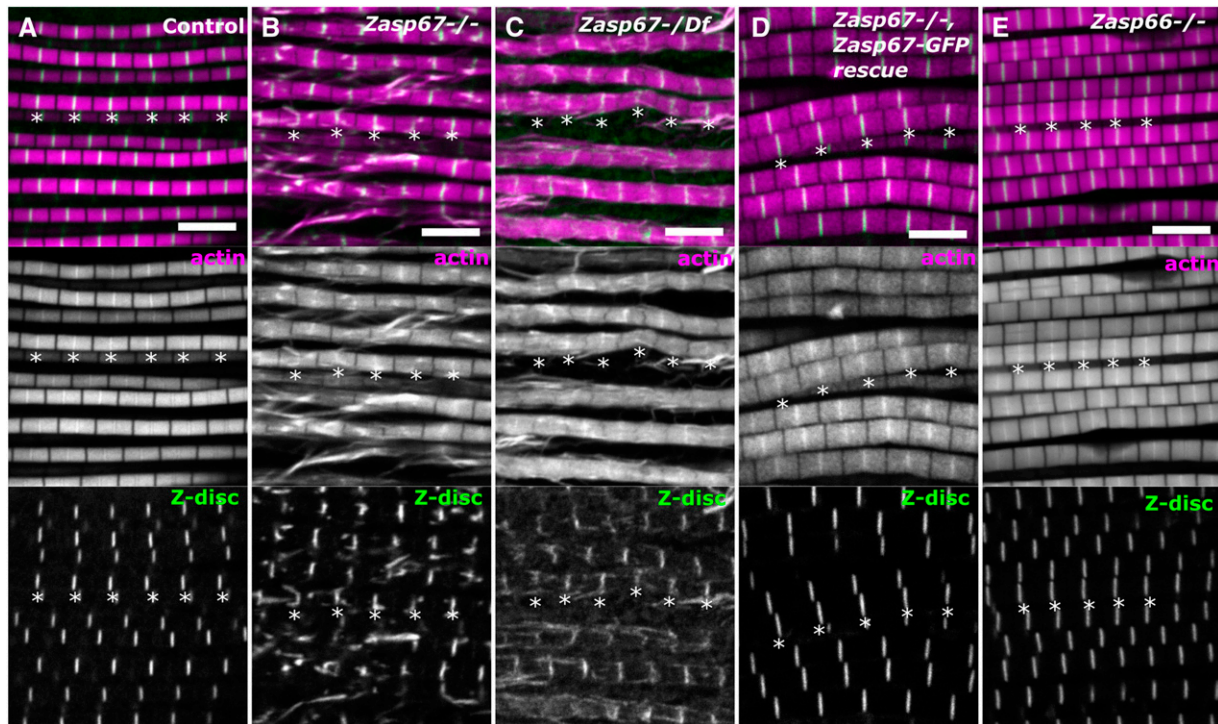


**Figure 6** Zasp67 mutants have defective indirect flight muscle myofibrils. Confocal images from the indirect flight muscles of 3-day-old flies from different genotypes. Actin filaments are stained with phalloidin (magenta in merged image) and *Zasp52-mCherry* was used to mark the Z-discs (green in merged image). Asterisks are drawn below selected Z-discs. (A) Control flies have a stereotypic sarcomere organization. (B) *Zasp67* null mutant indirect flight muscles showing broken and extended Z-discs. (C) Indirect flight muscles from a *Zasp67* mutant transheterozygous over a deficiency uncovering the *Zasp67* locus. (D) *Zasp67* null mutant indirect flight muscles with a *Zasp67-GFP* rescue construct. (E) *Zasp66* null mutant indirect flight muscles showing no obvious phenotypes. Bar, 5  $\mu\text{m}$ .

To confirm the *Zasp67* phenotype, we quantified the ratio of abnormal to normal Z-discs per image in wild type, *Zasp67*, *Zasp67/Df(3L)BSC393*, and *Zasp67-GFP*-rescued flies (Figure S3, A and D). We also further subdivided abnormal Z-discs into extended Z-discs (Figure S3, B and E) and broken Z-discs (Figure S3, C and F). In all cases, *Zasp67* mutant and *Zasp67/Df(3L)BSC393* show similar defects, which can be rescued by *Zasp67-GFP*. Extended Z-discs are more common than broken Z-discs (Figure S3, E and F).

Finally, we wanted to know if the *Zasp67* null mutant phenotype arises already during development, similar to the *Zasp52* and *Zasp66* RNAi phenotypes (Katzemich *et al.* 2013). We therefore stained pupal indirect flight muscles shortly before eclosion, when muscles have not yet been used for flying, at 96 hr after puparium formation. At this stage, no defects are visible compared to the wild type (Figure 7A). Abnormal Z-discs become first clearly apparent in 2-day-old flies (Figure 7B). 7 day-old flies have more severe defects with more frayed myofibrils, showing a phenotype progression with age (Figure 7C).

Altogether, these data indicate that *Zasp67* is required for the maintenance of indirect flight muscles rather than for sarcomere assembly during pupal development. In addition, *Zasp67* plays a more important role in myofibril stability and maintenance of adult indirect flight muscles than *Zasp66*.

## Discussion

Here, we have analyzed the evolutionary origin of *Zasp66* and *Zasp67* and their function in muscle development. We show that *Zasp67* functions in indirect flight muscle maintenance in *D. melanogaster*, whereas its paralog *Zasp66* functions in all muscles with only minor functions in indirect flight muscles.

### The evolutionary origin of *Zasp66* and *Zasp67*

*Zasp52* has a PDZ domain and four LIM domains and is the evolutionarily oldest member of the Alp/Enigma family in insects, because orthologs can be found in all metazoans and even in some unicellular eukaryotes (Steinmetz *et al.* 2012). In contrast, *Zasp66* is a duplication of *Zasp52* that we could detect only in insect species (Figure 1). *Zasp67* is a more recent duplication of *Zasp52*, and can be found only in a subset of insect orders with indirect flight muscles (Figure 1).

Gene duplication is known to be an important mechanism for the evolution of novel or specialized gene functions by providing new genetic material for evolutionary forces to act on (Zhang 2003). Indeed, large proportions of genes in all three domains of life were generated by gene duplication, including 20% of the genes found in *D. melanogaster* (Gu *et al.* 2002). The duplication of a gene frees one redundant copy to diverge and adopt either a partially or completely different function. Otherwise, the redundant copy

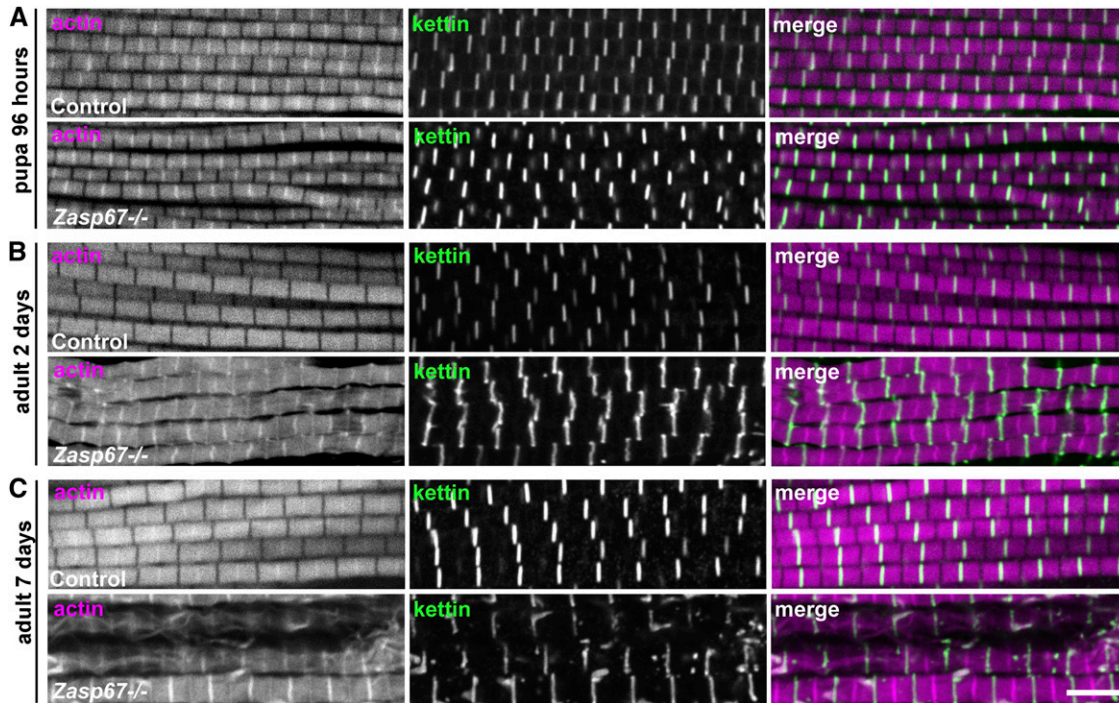


**Figure 7** Zasp67 is required for myofibril maintenance rather than development. Confocal images of indirect flight muscles at different life stages. Actin filaments are stained with phalloidin (magenta in merged image) and Z-discs were labeled with anti-kettin (green in merged image). (A) Indirect flight muscles 96 hr after puparium formation (APF). *Zasp67* null mutant muscles exhibit no phenotype compared to the wild-type control. (B) Indirect flight muscles of 2-day-old flies. At this stage, *Zasp67* null mutant muscles present abnormal Z-discs for the first time. (C) Indirect flight muscles of 7-day-old flies. At this stage, a greater number of frayed myofibrils is present in *Zasp67* null mutant flies. Bar, 5  $\mu$ m.

disappears by the accumulation of mutations, because it is unlikely that two genes with identical functions are maintained in a genome (Zhang 2003). As we do not know the ancestral function of Zasp52 in arthropods before Zasp66 and Zasp67 evolved, we cannot rigorously evaluate the evolutionary trajectories of Zasp66 and Zasp67. However, based on the functional data, we propose the following scenario for Zasp66 and Zasp67 in *D. melanogaster*: Zasp66 expression and localization is identical to Zasp52 (Figure 1 and Figure 3) (Hudson *et al.* 2008), and some of its functions residing in the PDZ domain, like  $\alpha$ -actinin binding, are conserved with Zasp52 (Katzemich *et al.* 2013). In addition, RNAi knock-down indicates partial redundancy of Zasp66 and Zasp67 with Zasp52 (Katzemich *et al.* 2013). The domain organization of Zasp66 is conserved across orthologs of different species, but Zasp66 orthologs consistently lack the three C-terminal LIM domains. This suggests that Zasp66 carries out distinct functions related to the absence of LIM domains.

For Zasp67, we observe a spatially and temporally restricted expression in indirect flight muscles (Figure 3). In addition, Zasp67 has a strong role in myofibril maintenance, but does not appear to be required for pupal myofibril assembly (Figure 7). This sets Zasp67 apart from Zasp66 and Zasp52, which are both required for pupal myofibril assembly (Katzemich *et al.* 2013), and could be a reason for why *D. melanogaster* Zasp67 was retained after duplication. On the other hand, most Zasp67 orthologs in other species are

highly diverse, with different orthologs having acquired different additional protein domains not usually found in Alp/Enigma family proteins (Figure 2, C–E). As we found Zasp67 orthologs only in some insects with indirect flight muscles, Zasp67 may have been more widespread initially, and may have been lost from several insect orders. Other Zasp67 orthologs may have additionally acquired different expression patterns, making them function in different muscles or even different tissues. We therefore propose that, upon the duplication event, most Zasp67 orthologs either acquired novel functions depending on which protein domains they have gained, or they disappeared by the accumulation of mutations. Given that Zasp52 has so many different splice isoforms, it is surprising that they are not sufficient for all muscle type-specific functions. It suggests as yet undiscovered functional constraints on Zasp52 evolution that led to the retention of Zasp66 and Zasp67 without LIM domains.

In *D. melanogaster*, Zasp67 appears to function exclusively in myofibril stabilization of indirect flight muscles, to a certain degree in conjunction with Zasp52 and Zasp66. This maintenance defect of indirect flight muscles of *Zasp67* mutants is stronger than that of *Zasp66*, and can easily be observed by confocal microscopy (Figure 6 and Figure 7). In contrast, the indirect flight muscle phenotype of *Zasp66* is milder, but appears already during pupal stages (Katzemich *et al.* 2013), suggesting that Zasp67 has taken over some or

most of the maintenance roles in indirect flight muscles that are carried out by Zasp66 or Zasp52 in other species.

In summary, Zasp67 has acquired specialized functions in *D. melanogaster* in stabilizing indirect flight muscles, whereas its paralog Zasp66 appears to function together with Zasp52 in mediating general functions of myofibril assembly.

## Acknowledgments

We thank the Bloomington *Drosophila* stock center, Vienna *Drosophila* Resource Center, and the Children's Hospital Oakland Research Institute for materials and the Cell Imaging and Analysis Network (CIAN) imaging facility for providing access to confocal microscopy. This work was supported by operating grants MOP-142475 and PJT-155995 from the Canadian Institutes of Health Research and by RGPIN (Research Grants Program Individual) 2016-06793 from the Natural Sciences and Engineering Research Council of Canada.

## Literature Cited

- Boc, A., A. B. Diallo, and V. Makarenkov, 2012 T-REX: a web server for inferring, validating and visualizing phylogenetic trees and networks. *Nucleic Acids Res.* 40: W573–W579. <https://doi.org/10.1093/nar/gks485>
- Brown, J. B., N. Boley, R. Eisman, G. E. May, M. H. Stoiber *et al.*, 2014 Diversity and dynamics of the *Drosophila* transcriptome. *Nature* 512: 393–399. <https://doi.org/10.1038/nature12962>
- Chechenova, M. B., A. L. Bryantsev, and R. M. Cripps, 2013 The *Drosophila* Z-disc protein Z(210) is an adult muscle isoform of Zasp52, which is required for normal myofibril organization in indirect flight muscles. *J. Biol. Chem.* 288: 3718–3726. <https://doi.org/10.1074/jbc.M112.401794>
- Cheng, H., K. Kimura, A. K. Peter, L. Cui, K. Ouyang *et al.*, 2010 Loss of enigma homolog protein results in dilated cardiomyopathy. *Circ. Res.* 107: 348–356. <https://doi.org/10.1161/CIRCRESAHA.110.218735>
- Cook, R. K., S. J. Christensen, J. A. Deal, R. A. Coburn, M. E. Deal *et al.*, 2012 The generation of chromosomal deletions to provide extensive coverage and subdivision of the *Drosophila melanogaster* genome. *Genome Biol.* 13: R21. <https://doi.org/10.1186/gb-2012-13-3-r21>
- D'Cruz, R., P. J. Plant, L. A. Pablo, S. Lin, J. Chackowicz *et al.*, 2016 PDLIM7 is a novel target of the ubiquitin ligase Nedd4-1 in skeletal muscle. *Biochem. J.* 473: 267–276. <https://doi.org/10.1042/BJ20150222>
- Deora, T., N. Gundiah, and S. P. Sane, 2017 Mechanics of the thorax in flies. *J. Exp. Biol.* 220: 1382–1395. <https://doi.org/10.1242/jeb.128363>
- Faulkner, G., A. Pallavicini, E. Formentin, A. Comelli, C. Ievolella *et al.*, 1999 ZASP: a new Z-band alternatively spliced PDZ-motif protein. *J. Cell Biol.* 146: 465–475. <https://doi.org/10.1083/jcb.146.2.465>
- Gentleman, R. C., V. J. Carey, D. M. Bates, B. Bolstad, M. Dettling *et al.*, 2004 Bioconductor: open software development for computational biology and bioinformatics. *Genome Biol.* 5: R80. <https://doi.org/10.1186/gb-2004-5-10-r80>
- González-Morales, N., T. K. Holenka, and F. Schöck, 2017 Filamin actin-binding and titin-binding fulfill distinct functions in Z-disc cohesion. *PLoS Genet.* 13: e1006880. <https://doi.org/10.1371/journal.pgen.1006880>
- Graveley, B. R., A. N. Brooks, J. W. Carlson, M. O. Duff, J. M. Landolin *et al.*, 2011 The developmental transcriptome of *Drosophila melanogaster*. *Nature* 471: 473–479. <https://doi.org/10.1038/nature09715>
- Gu, Z., A. Cavalcanti, F. C. Chen, P. Bouman, and W. H. Li, 2002 Extent of gene duplication in the genomes of *Drosophila*, nematode, and yeast. *Mol. Biol. Evol.* 19: 256–262. <https://doi.org/10.1093/oxfordjournals.molbev.a004079>
- Guindon, S., and O. Gascuel, 2003 A simple, fast, and accurate algorithm to estimate large phylogenies by maximum likelihood. *Syst. Biol.* 52: 696–704. <https://doi.org/10.1080/10635150390235520>
- Han, H. F., and M. C. Beckerle, 2009 The ALP-Enigma protein ALP-1 functions in actin filament organization to promote muscle structural integrity in *Caenorhabditis elegans*. *Mol. Biol. Cell* 20: 2361–2370. <https://doi.org/10.1091/mbc.e08-06-0584>
- Hudson, A. M., L. N. Petrella, A. J. Tanaka, and L. Cooley, 2008 Mononuclear muscle cells in *Drosophila* ovaries revealed by GFP protein traps. *Dev. Biol.* 314: 329–340. <https://doi.org/10.1016/j.ydbio.2007.11.029>
- Jani, K., and F. Schöck, 2007 Zasp is required for the assembly of functional integrin adhesion sites. *J. Cell Biol.* 179: 1583–1597. <https://doi.org/10.1083/jcb.200707045>
- Jo, K., B. Rutten, R. C. Bunn, and D. S. Bredt, 2001 Actinin-associated LIM protein-deficient mice maintain normal development and structure of skeletal muscle. *Mol. Cell. Biol.* 21: 1682–1687. <https://doi.org/10.1128/MCB.21.5.1682-1687.2001>
- Kadmas, J. L., and M. C. Beckerle, 2004 The LIM domain: from the cytoskeleton to the nucleus. *Nat. Rev. Mol. Cell Biol.* 5: 920–931. <https://doi.org/10.1038/nrm1499>
- Katzemich, A., J. Y. Long, K. Jani, B. R. Lee, and F. Schöck, 2011 Muscle type-specific expression of Zasp52 isoforms in *Drosophila*. *Gene Expr. Patterns* 11: 484–490. <https://doi.org/10.1016/j.gexp.2011.08.004>
- Katzemich, A., N. Kreisköther, A. Alexandrovich, C. Elliott, F. Schöck *et al.*, 2012 The function of the M-line protein obscurin in controlling the symmetry of the sarcomere in the flight muscle of *Drosophila*. *J. Cell Sci.* 125: 3367–3379. <https://doi.org/10.1242/jcs.097345>
- Katzemich, A., K. A. Liao, S. Czerniecki, and F. Schöck, 2013 Alp/Enigma family proteins cooperate in Z-disc formation and myofibril assembly. *PLoS Genet.* 9: e1003342. <https://doi.org/10.1371/journal.pgen.1003342>
- Koch, B. J., J. F. Ryan, and A. D. Baxeivanis, 2012 The diversification of the LIM superclass at the base of the metazoa increased subcellular complexity and promoted multicellular specialization. *PLoS One* 7: e33261. <https://doi.org/10.1371/journal.pone.0033261>
- Kondo, S., and R. Ueda, 2013 Highly improved gene targeting by germline-specific Cas9 expression in *Drosophila*. *Genetics* 195: 715–721. <https://doi.org/10.1534/genetics.113.156737>
- Lemke, S. B., and F. Schnorrer, 2017 Mechanical forces during muscle development. *Mech. Dev.* 144: 92–101. <https://doi.org/10.1016/j.mod.2016.11.003>
- Liao, K. A., N. González-Morales, and F. Schöck, 2016 Zasp52, a core Z-disc protein in *Drosophila* indirect flight muscles, interacts with alpha-actinin via an extended PDZ domain. *PLoS Genet.* 12: e1006400. <https://doi.org/10.1371/journal.pgen.1006400>
- Luck, K., S. Charbonnier, and G. Travé, 2012 The emerging contribution of sequence context to the specificity of protein interactions mediated by PDZ domains. *FEBS Lett.* 586: 2648–2661. <https://doi.org/10.1016/j.febslet.2012.03.056>
- Luther, P. K., 2009 The vertebrate muscle Z-disc: sarcomere anchor for structure and signalling. *J. Muscle Res. Cell Motil.* 30: 171–185. <https://doi.org/10.1007/s10974-009-9189-6>
- Marchler-Bauer, A., M. K. Derbyshire, N. R. Gonzales, S. Lu, F. Chitsaz *et al.*, 2015 CDD: NCBI's conserved domain database. *Nucleic Acids Res.* 43: D222–D226. <https://doi.org/10.1093/nar/gku1221>

- Marygold, S. J., M. A. Crosby, J. L. Goodman, and F. Consortium, 2016 Using FlyBase, a database of *Drosophila* genes and genomes. *Methods Mol. Biol.* 1478: 1–31. [https://doi.org/10.1007/978-1-4939-6371-3\\_1](https://doi.org/10.1007/978-1-4939-6371-3_1)
- McKeown, C. R., H. F. Han, and M. C. Beckerle, 2006 Molecular characterization of the *Caenorhabditis elegans* ALP/Enigma gene alp-1. *Dev. Dyn.* 235: 530–538. <https://doi.org/10.1002/dvdy.20633>
- Misof, B., S. Liu, K. Meusemann, R. S. Peters, A. Donath *et al.*, 2014 Phylogenomics resolves the timing and pattern of insect evolution. *Science* 346: 763–767. <https://doi.org/10.1126/science.1257570>
- Mu, Y., R. Jing, A. K. Peter, S. Lange, L. Lin *et al.*, 2015 Cypher and Enigma homolog protein are essential for cardiac development and embryonic survival. *J. Am. Heart Assoc.* 4: e001950. <https://doi.org/10.1161/JAHA.115.001950>
- Nahabedian, J. F., H. Qadota, J. N. Stirman, H. Lu, and G. M. Benian, 2012 Bending amplitude - a new quantitative assay of *C. elegans* locomotion: identification of phenotypes for mutants in genes encoding muscle focal adhesion components. *Methods* 56: 95–102. <https://doi.org/10.1016/j.ymeth.2011.11.005>
- Papadopoulos, J. S., and R. Agarwala, 2007 COBALT: constraint-based alignment tool for multiple protein sequences. *Bioinformatics* 23: 1073–1079. <https://doi.org/10.1093/bioinformatics/btm076>
- Paradis, E., J. Claude, and K. Strimmer, 2004 APE: analyses of phylogenetics and evolution in R language. *Bioinformatics* 20: 289–290. <https://doi.org/10.1093/bioinformatics/btg412>
- Pashmforoush, M., P. Pomiès, K. L. Peterson, S. Kubalak, J. Ross, Jr. *et al.*, 2001 Adult mice deficient in actinin-associated LIM-domain protein reveal a developmental pathway for right ventricular cardiomyopathy. *Nat. Med.* 7: 591–597. <https://doi.org/10.1038/87920>
- Sarov, M., C. Barz, H. Jambor, M. Y. Hein, C. Schmied *et al.*, 2016 A genome-wide resource for the analysis of protein localisation in *Drosophila*. *eLife* 5: e12068. <https://doi.org/10.7554/eLife.12068>
- Schindelin, J., I. Arganda-Carreras, E. Frise, V. Kaynig, M. Longair *et al.*, 2012 Fiji: an open-source platform for biological-image analysis. *Nat. Methods* 9: 676–682. <https://doi.org/10.1038/nmeth.2019>
- Sheikh, F., M. L. Bang, S. Lange, and J. Chen, 2007 “Z”eroing in on the role of Cypher in striated muscle function, signaling, and human disease. *Trends Cardiovasc. Med.* 17: 258–262. <https://doi.org/10.1016/j.tcm.2007.09.002>
- Shieh, P. B., 2013 Muscular dystrophies and other genetic myopathies. *Neurol. Clin.* 31: 1009–1029. <https://doi.org/10.1016/j.ncl.2013.04.004>
- Steinmetz, P. R. H., J. E. M. Kraus, C. Larroux, J. U. Hammel, A. Amon-Hassenzahl *et al.*, 2012 Independent evolution of striated muscles in cnidarians and bilaterians. *Nature* 487: 231–234. <https://doi.org/10.1038/nature11180>
- Torrado, M., V. V. Senatorov, R. Trivedi, R. N. Fariss, and S. I. Tomarev, 2004 Pdlim2, a novel PDZ-LIM domain protein, interacts with alpha-actinins and filamin A. *Invest. Ophthalmol. Vis. Sci.* 45: 3955–3963. <https://doi.org/10.1167/iovs.04-0721>
- Vallenius, T., K. Luukko, and T. P. Mäkelä, 2000 CLP-36 PDZ-LIM protein associates with nonmuscle alpha-actinin-1 and alpha-actinin-4. *J. Biol. Chem.* 275: 11100–11105. <https://doi.org/10.1074/jbc.275.15.11100>
- Vallenius, T., B. Scharm, A. Vesikansa, K. Luukko, R. Schäfer *et al.*, 2004 The PDZ-LIM protein RIL modulates actin stress fiber turnover and enhances the association of alpha-actinin with F-actin. *Exp. Cell Res.* 293: 117–128. <https://doi.org/10.1016/j.yexcr.2003.09.004>
- van der Meer, D. L., I. J. Marques, J. T. Leito, J. Besser, J. Bakkers *et al.*, 2006 Zebrafish cypher is important for somite formation and heart development. *Dev. Biol.* 299: 356–372. <https://doi.org/10.1016/j.ydbio.2006.07.032>
- Venken, K. J., K. L. Schulze, N. A. Haelterman, H. Pan, Y. He *et al.*, 2011 MiMIC: a highly versatile transposon insertion resource for engineering *Drosophila melanogaster* genes. *Nat. Methods* 8: 737–743. <https://doi.org/10.1038/nmeth.1662>
- Xiao, Y. S., F. Schöck, and N. González-Morales, 2017 Rapid IFM dissection for visualizing fluorescently tagged sarcomeric proteins. *Bio Protoc.* 7: e2606. <https://doi.org/10.21769/Bio-Protoc.2606>
- Zhang, J., 2003 Evolution by gene duplication: an update. *Trends Ecol. Evol.* 18: 292–298. [https://doi.org/10.1016/S0169-5347\(03\)00033-8](https://doi.org/10.1016/S0169-5347(03)00033-8)
- Zheng, M., H. Cheng, I. Banerjee, and J. Chen, 2010 ALP/Enigma PDZ-LIM domain proteins in the heart. *J. Mol. Cell Biol.* 2: 96–102. <https://doi.org/10.1093/jmcb/mjp038>
- Zhou, Q., P. H. Chu, C. Huang, C. F. Cheng, M. E. Martone *et al.*, 2001 Ablation of Cypher, a PDZ-LIM domain Z-line protein, causes a severe form of congenital myopathy. *J. Cell Biol.* 155: 605–612. <https://doi.org/10.1083/jcb.200107092>

Communicating editor: M. Wolfner